# New Control of PV Solar Farm as STATCOM (PV-STATCOM) for Increasing Grid Power Transmission Limits During Night and Day

Rajiv K. Varma, *Senior Member, IEEE*, Shah Arifur Rahman, *Member, IEEE*, and Tim Vanderheide, *Member, IEEE*

***Abstract*—This paper presents a novel concept of utilizing a photovoltaic (PV) solar farm inverter as STATCOM, called PV-STATCOM, for improving stable power transfer limits of the interconnected transmission system. The entire inverter rating of the PV solar farm, which remains dormant during nighttime, is utilized with voltage and damping controls to enhance stable power transmission limits. During daytime, the inverter capacity left after real power production is used to accomplish the aforementioned objective. Transient stability studies are conducted on a realistic single machine infinite bus power system having a midpoint located PV-STATCOM using EMTDC/PSCAD simulation software. The PV-STATCOM improves the stable transmission limits substantially in the night and in the day even while generating large amounts of real power. Power transfer increases are also demonstrated in the same power system for: 1) two solar farms operating as PV-STATCOMs and 2) a solar farm as PV-STATCOM and an inverter-based wind farm with similar STATCOM controls. This novel utilization of a PV solar farm asset can thus improve power transmission limits which would have otherwise required expensive additional equipment, such as series/shunt capacitors or separate flexible ac transmission system controllers.**

***Index Terms*—Damping control, flexible ac transmission systems (FACTS), inverter, photovoltaic solar power systems, reactive power control, STATCOM, transmission capacity, voltage control, wind power system.**

## I. Introduction

FLEXIBLE AC transmission system (FACTS) controllers are being increasingly considered to increase the available power transfer limits/capacity (ATC) of existing transmission lines [1]–[4], globally. New research has been reported on the nighttime usage of a photovoltaic (PV) solar farm (when it is normally dormant) where a PV solar farm is utilized as a STATCOM–a FACTS controller, for performing voltage control, thereby improving system performance and increasing grid connectivity of neighboring wind farms [5], [6]. New voltage control has also been proposed on a PV solar farm to act as a STATCOM for improving the power transmission capacity [7]. Although, [8] and [9] have proposed voltage-control functionality with PV systems, none have utilized the PV system for power transfer limit improvement. A full converter-based wind turbine generator has recently been provided with FACTS capabilities for improved response during faults and fault ride-through capabilities [10].

This paper proposes novel voltage control, together with auxiliary damping control, for a grid-connected PV solar farm inverter to act as a STATCOM both during night and day for increasing transient stability and consequently the power transmission limit. This technology of utilizing a PV solar farm as a STATCOM is called "PV-STATCOM." It utilizes the entire solar farm inverter capacity in the night and the remainder inverter capacity after real power generation during the day, both of which remain unused in conventional solar farm operation. Similar STATCOM control functionality can also be implemented in inverter-based wind turbine generators during no-wind or partial wind scenarios for improving the transient stability of the system. Studies are performed for two variants of a single-machine infinite bus (SMIB) system. One SMIB system uses only a single PV solar farm as PV-STATCOM connected at the midpoint whereas the other system uses a combination of a PV-STATCOM and another PV-STATCOM or an inverter-based wind distributed generator (DG) with similar STATCOM functionality. Three-phase fault studies are conducted using the electromagnetic transient software EMTDC/PSCAD, and the improvement in the stable power transmission limit is investigated for different combinations of STATCOM controllers on the solar and wind farm inverters, both during night and day.

Section II describes the study systems. The results for various fault studies are presented in Section III. The performances of different proposed controls during daytime and nighttime are presented. The implications of implementing this new PV-STATCOM technology on large-scale solar systems are described in Section IV, while the conclusions are presented in Section IV.

## II. System Models

The single-line diagrams of two study systems: Study System 1 and Study System 2 are depicted in Fig. 1(a) and (b),

Manuscript received December 04, 2011; revised June 25, 2012; accepted March 07, 2013. Date of publication December 05, 2014; date of current version March 20, 2015. This work was supported in part by Ontario Centres of Excellence (OCE), Bluewater Power, Sarnia, and Hydro One under Grants WE-SP109-E50712-08 and CR-SG30-11182-11 and in part by NSERC. Paper no. TPWRD-01030-2011.

R. K. Varma and S. A. Rahman are with the Department of Electrical and Computer Engineering, University of Western Ontario, London, ON N6A 5B9, Canada (e-mail: rkvarma@uwo.ca; srahma32@uwo.ca).

T. Vanderheide is with Bluewater Power Renewable Energy Inc., Sarnia, ON N7T 7L6 Canada (e-mail: TVanderheide@bluewaterpower.com).

Color versions of one or more of the figures in this paper are available online at http://ieeexplore.ieee.org.

Digital Object Identifier 10.1109/TPWRD.2014.2375216

respectively. Both systems are single-machine infinite bus (SMIB) systems where a large equivalent synchronous generator (1110 MVA) supplies power to the infinite bus over a 200-km, 400-kV transmission line. This line length is typical of a long line carrying bulk power in Ontario. In Study System 1, a 100-MW PV solar farm (DG) as STATCOM (PV-STATCOM) is connected at the midpoint of the transmission line. In Study System 2, two 100-MVA inverter-based distributed generators (DGs) are connected at 1/3 (bus 5) and 2/3 (bus 6) of the line length from the synchronous generator. The DG connected at bus 6 is a PV-STATCOM and the other DG at bus 5 is either a PV-STATCOM or a wind farm with STATCOM functionality. In this case, the wind farm employs permanent-magnet synchronous generator (PMSG)-based wind turbine generators with a full ac-dc-ac converter. It is understood that the solar DG and wind DG employ several inverters. However, for this analysis, each DG is considered to have a single equivalent inverter with the rating equal to the total rating of solar DG or wind DG, respectively. The wind DG and solar DG are considered to be of the same rating, hence, they can be interchanged in terms of location depending upon the studies being performed. Fig. 2 presents the block diagrams of various subsystems of two equivalent DGs. All of the system parameters are given in [1].

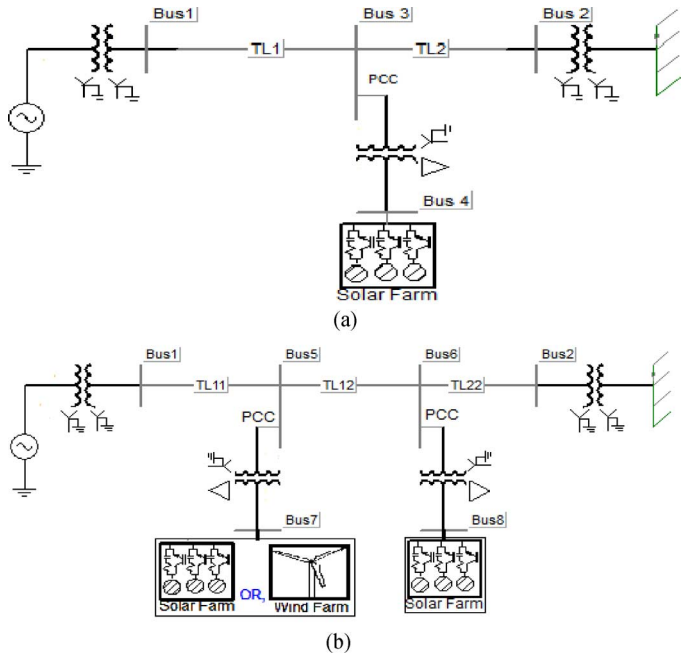


Fig. 1. Single-line diagram of (a) study system I with a single solar farm (DG) and (b) study system II with a solar farm (DG) and a solar/wind farm (DG).

### A. System Model

The synchronous generator is represented by a detailed sixth-order model and a DC1A-type exciter [1]. The transmission-line segments TL1, TL2, TL11, TL12, and TL22, shown in Fig. 1, are represented by lumped pi-circuits. The PV solar DG, as shown in Fig. 2, is modeled as an equivalent voltage-source inverter along with a controlled current source as the dc source which follows the I-V characteristics of PV panels [11]. The wind DG is likewise modeled as an equivalent voltage-source inverter. In the solar DG, dc power is provided by the solar panels, whereas in the full-converter-based wind DG, dc power comes out of a controlled ac–dc rectifier connected to the PMSG wind turbines, depicted as "wind Turbine-Generator-Rectifier (T-G-R)." The dc power produced by each DG is fed into the dc bus of the corresponding inverter, as illustrated in Fig. 2. A maximum power point tracking (MPPT) algorithm based on an incremental conductance algorithm [12] is used to operate the solar DGs at its maximum power point all of the time and is integrated with the inverter controller [11]. The wind DG is also assumed to operate at its maximum power point, since this proposed control utilizes only the inverter capacity left after the maximum power point operation of the solar DG and wind DG.

For PV-STATCOM operation during nighttime, the solar panels are disconnected from the inverter and a small amount of real power is drawn from the grid to charge the dc capacitor. The voltage-source inverter in each DG is composed of six insulated-gate bipolar transistors (IGBTs) and associated snubber circuits as shown in Fig. 2. An appropriately large dc capacitor of size 200 Farad is selected to reduce the dc side ripple [13]. Each phase has a pair of IGBT devices which converts the dc voltage into a series of variable-width pulsating voltages, using the sinusoidal pulsewidth modulation (SPWM) technique [14]. An L-C-L filter [13] is also connected at the inverter ac side.

### B. Control System

*1) Conventional Reactive Power Control:* The conventional reactive power control only regulates the reactive power output of the inverter such that it can perform unity power factor operation along with dc-link voltage control [15]. The switching signals for the inverter switching are generated through two current control loops in d-q-0 coordinate system [15], [16]. The inverter operates in a conventional controller mode only provided that "Switch-2" is in the "OFF" position. In this simulation, the voltage vector is aligned with the quadrature axis, that is, $V_d = 0$ [15], [16], hence, $Q_{\rm ref}$ is only proportional to $\rm I_d$ which sets the reference $I_{d\_\rm ref}$ for the upper control loop involving PI1. Meanwhile, the quadrature axis component $\rm I_q$ is used for dc-link voltage control through two PI controllers (PI-2 and PI-3) [14], [16] shown in Fig. 2(b) according to the setpoint voltage provided by the MPPT and and injects all available real power "P" to the network [15]. To generate the proper IGBT switching signals (gt1, gt2, gt3, gt4, gt5, gt6), the d–q components (md and mq) of the modulating signal are converted into three-phase sinusoidal modulating signals and compared with a high-frequency (5-kHz) fixed magnitude triangular wave or carrier signal.

*2) PCC Voltage Control:* In the *PCC voltage control* mode of operation, the PCC voltage is controlled through reactive power exchange between the DG inverter and the grid. The conventional "$Q$" control channel is replaced by the PCC voltage controller in Fig. 2(b), simply by switching "Switch-1" to the position "A." Hence, the measured signal $V_{\rm PCC}$ at the PCC is compared with the preset reference value $V_{PCC\_\rm ref}$ and is passed through the PI regulator, PI-4, to generate $I_{d\_\rm ref}$.

The rest of the controller remains unchanged. The upper current control loop is used to regulate the PCC voltage whereas the lower current control loop is used for dc voltage control and

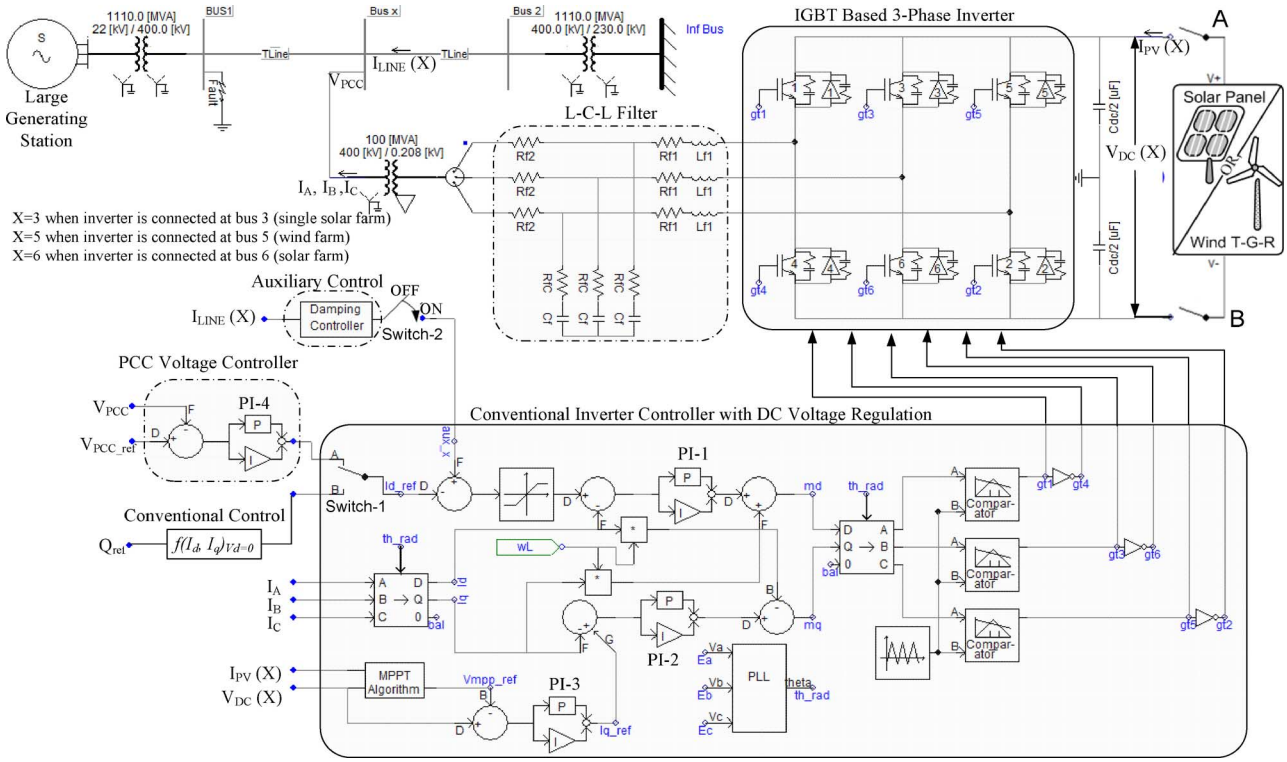


Fig. 2. Complete DG (solar/wind) system model with a damping controller and PCC voltage-control system.

as well as for the supply of DG power to the grid. The amount of reactive power flow from the inverter to the grid depends on setpoint voltage at the PCC. The parameters of the PCC voltage controller are tuned by a systematic trial-and-error method to achieve the fastest step response, least settling time, and a maximum overshoot of 10%–15%. The parameters of all controllers are given in the Appendix.

*3) Damping Control:* A novel auxiliary *damping controller* is added to the PV control system and shown in Fig. 2. (b). This controller utilizes line current magnitude as the control signal. The output of this controller is added with the signal $I_{d\_\mathrm{ref}}$. The transfer function of this damping controller is expressed as in [19]

$$F_D = G \cdot \frac{sT_w}{1+sT_w} \cdot \left(\frac{1+sT_1}{1+sT_2}\right). \tag{1}$$

The transfer function is comprised of a gain, a washout stage, and a first-order lead-lag compensator block. This controller is utilized to damp the rotor-mode oscillations of the synchronous generator and thereby improve system transient stability. The damping controller is activated by toggling "Switch-2" to the "ON" position. This damping controller can operate in conjunction with either the conventional reactive power control mode or with the PCC voltage-control mode by toggling "Switch-1" to position "B" or "A," respectively.

At first, the base-case generator operating power level is selected for performing the damping control design studies. This power level is considered equal to the transient stability limit of the system with the solar farm being disconnected at night. At this operating power level, if a three-phase fault occurs at Bus 1, the generator power oscillations decay with a damping ratio of 5%. The solar farm is now connected and operated in the PV-STATCOM mode. The parameters of the damping controller $F_D$ are selected as follows. The washout time constant $T_w$ is chosen to allow the generator electromechanical oscillations in the frequency range up to 2 Hz to pass through [19]. The gain G, time constants T1, and T2 are sequentially tuned to obtain the fastest settling time of the electromechanical oscillations at the base-case generator power level through repetitive PSCAD/EMTDC simulations. Thus, the best combination of the controller parameters is obtained with a systematic hit-and-trial technique, and the parameters are given in the Appendix. It is emphasized that these controller parameters are not optimal and better parameters could be obtained by following more rigorous control-design techniques [19], [20]. However, the objective of this paper is only to demonstrate a new concept of using a PV solar farm inverter as a STATCOM using these reasonably good controller parameters. In this controller, although the line current magnitude signal is used, other local or remote signals, which reflect the generator rotor-mode oscillations [1], may also be utilized.

## III. System Studies

Transient stability studies are carried out using PSCAD/EMTDC simulation software, for both the study systems during night and day, by applying a three-line-to-ground (3LG) fault at bus 1 for five cycles. The damping ratio is used to express the rate of decay of the amplitude of oscillation [20]. For an oscillatory mode having an eigenvalue of $\sigma + j\sigma$, the damping ratio $\xi$ is defined as

$$\xi = -\frac{\sigma}{\sqrt{\sigma^2+\omega^2}}, \quad \text{and} \quad \sigma = \frac{1}{\tau} \tag{2}$$

where $\tau$ is the time constant.

TABLE I
POWER FLOWS AND VOLTAGES FOR STUDY SYSTEM I FOR SOLAR DG WITH CONVENTIONAL REACTIVE POWER CONTROL AND PROPOSED DAMPING CONTROL BOTH DURING NIGHTTIME AND DAYTIME (Vg = 1.05 p.u.)

| Simulation Description | | Gen. Bus | PCC/Middle Bus (3) | | | Inf. Bus |
|---|---|---|---|---|---|---|
| | | Pg (MW) | Vpcc (pu) | Psolar (MW) | Qsolar (MVAr | Pinf (MW) |
| Nighttime | Conventional Operation of Solar DG | **731** | 1.010 | 0 | 0 | **-708** |
| | Solar DG with damping controller | **850** | 1.000 | -0.20 | 0.08 | **-819** |
| Daytime | Conventional Operation of Solar DG | **730** | 1.010 | **19.0** | -0.50 | **-725** |
| | | **719** | 1.008 | **91.0** | -0.20 | **-786** |
| | Solar DG with damping controller | **851** | 1.000 | **19.0** | -0.06 | **-839** |
| | | **861** | 0.994 | **91.0** | -0.20 | **-917** |

Therefore, for a 5% damping ratio of the rotor mode having an oscillation frequency of 0.95 Hz, as considered in this study, the postfault clearance settling time of the oscillations to come within 5% (typically within 3 times the time constant) of its steady-state value [1], [20] is almost 10 s. The peak overshoot of PCC voltage should also be limited within 1.1 p.u. of nominal voltage. The maximum stable generator power limit for the system is determined through transient stability studies for different modes of operation of the solar DG in study system 1, and those of the solar DG and the solar/winds DGs in study system 2.

### *A. Case Study 1: Power Transfer Limits in Study System 1*

*1) Conventional Reactive Power Control With Novel Damping Control:* In this study, the solar DG is assumed to operate with its conventional reactive power controller and the DG operates at near unity power factor. For the nighttime operation of solar DG, the dc sources (solar arrays) are disconnected, and the solar DG inverter is connected to the grid using appropriate controllers, as will be described. Power transmission limits are now determined for the following four cases. The stable power transmission limits obtained from transient stability studies and the corresponding load-flow results are presented in Table I where −ve Q represents the inductive power drawn and +ve Q represents the capacitive power injected into the network.

*Solar DG Operation During Night With Conventional Reactive Power Controllers:* The maximum stable power output from the generator $P_g$ is 731 MW when the solar DG is simply sitting idle during night and is disconnected from the network. This power-flow level is chosen to be the base value against which the improvements in power flow with different proposed controllers are compared and illustrated later in Table III. The real power from generator $P_g$ and that entering the infinite bus $P_{inf}$ for this fault study are shown in Fig. 3(a). The sending-end voltage at the generator is shown in Fig. 3(b) which shows a voltage overshoot of 1.1 p.u.

*Solar DG Operation During the Night With Damping Controllers:* The quantities $P_g$, $P_{inf}$, $P_{solar}$, and $Q_{solar}$ are illustrated in Fig. 4(a). The damping controller utilizes the full rating of the DG inverter at night to provide controlled reactive power $Q_{solar}$ and effectively damps the generator rotor-mode oscillations. The voltages at generator bus $V_g$ and at the PCC bus $V_{rms(PCC)}$ are depicted in Fig. 4(b). A very small amount of negative power flow from the solar farm $P_{solar}$ is observed during nighttime. This reflects the losses in the inverter IGBT switches as well as transformer and filter resistances caused

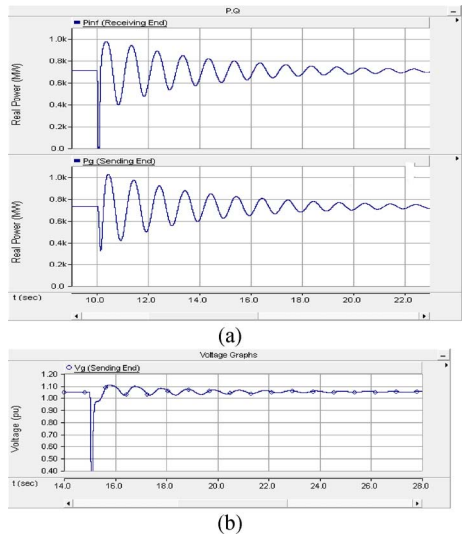


Fig. 3. (a) Maximum nighttime power transfer (731 MW) from the generator when solar DG remains idle. (b) Voltage at the generator terminal.

TABLE II
POWER FLOWS AND VOLTAGES FOR STUDY SYSTEM I FOR SOLAR DG WITH THE PROPOSED PCC VOLTAGE CONTROL AND DAMPING CONTROL DURING NIGHTTIME AND DAYTIME (Vg = 1.05 p.u.)

| Simulation Description | | Gen. Bus | PCC/Middle Bus (3) | | | Inf. Bus |
|---|---|---|---|---|---|---|
| | | Pg (MW) | Vpcc (pu) | Psolar (MW) | Qsolar (MVAr) | Pinf (MW) |
| Nighttime | Solar DG with voltage controller | **789** | 0.988 | -1.5 | -95.8 | **-761** |
| | | **824** | 0.990 | -0.8 | -66.0 | **-793** |
| | | **830** | 1.000 | -0.3 | -9.5 | **-801** |
| | | **833** | 1.010 | -0.5 | 46.8 | **-803** |
| | | **803** | 1.022 | -1.5 | 99.0 | **-775** |
| | Solar DG with both voltage and damping controller | **855** | 1.000 | -0.3 | 4.0 | **-824** |
| | | **899** | 1.010 | -1.2 | 85.0 | **-866** |
| Daytime | Solar DG with voltage controller | **781** | 0.990 | **19.0** | -90.0 | **-773** |
| | | **815** | 1.000 | **19.0** | -13.7 | **-804** |
| | | **782** | 1.021 | **19.0** | 86.0 | **-775** |
| | | **726** | 0.99 | **91.0** | -43.0 | **-792** |
| | | **719** | 1.000 | **91.0** | -44.0 | **-786** |
| | Solar DG with both voltage and damping controller | **823** | 1.000 | **19.0** | -9.0 | **-813** |
| | | **755** | 1.000 | **91.0** | -41.0 | **-817** |

TABLE III
INCREASE IN THE STABLE POWER TRANSFER LIMIT (IN MEGAWATTS) FOR STUDY SYSTEM I WITH DIFFERENT PV-STATCOM CONTROLS

| PV STATCOM CONTROL | NIGHT | DAY | |
|---|---|---|---|
| | | Solar Power Output 19 MW | Solar Power Output 91 MW |
| Voltage Control | 102 | 85 | 7 |
| Damping Control | 119 | **121** | **142** |
| Voltage Control with Damping Control | **168** | 93 | 36 |

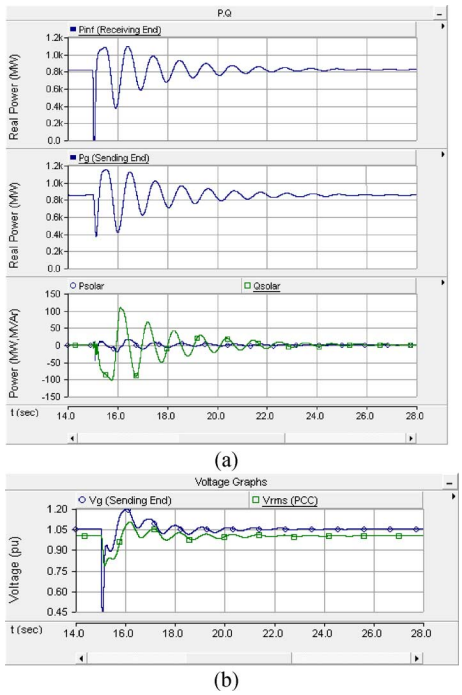


Fig. 4. (a) Maximum nighttime power transfer (850 MW) from the generator with solar DG using the damping controller. (b) Voltages at the generator terminal and DG PCC.

by the flow of real current from the grid into the solar farm inverter to charge the dc-link capacitor and maintain its voltage constant while operating the PV inverter as STATCOM with the damping controller (or even with a voltage controller). During nighttime, the reference dc-link voltage $V_{mpp\_ref}$ is chosen around the typical daytime-rated maximum powerpoint (MPP) voltage.

The oscillations in the solar PV power output during nighttime, as seen in Fig. 4, are due to the active power exchanged by the solar inverter both during the charge and discharge cycles in trying to maintain a constant voltage across the dc-link capacitor, thereby enabling the inverter to operate as a STATCOM.

*Solar DG Operation During the Day With a Conventional Reactive Power Controller:* The conventional control of a PV solar DG does not seem to alter the stable transmission limit in any appreciable manner.

*Solar DG Operation During the Day With a Damping Controller:* The quantities $\mathrm{P_g}$, $\mathrm{P_{inf}}$, $\mathrm{P_{solar}}$, and $\mathrm{Q_{solar}}$ are shown for the cases without the damping controller and with the damping controller in Figs. 5 and 6, respectively. The available inverter capacity after real power generation of 91 MW is $Q = \sqrt{(S^2 - P^2)} = 41.5$ MVAr, which is used for damping oscillations during the day.

The power transfer capacity increase in the daytime is expected to be lower than the nighttime, since only a part of the total inverter capacity is available for damping control during the day. However, it is noticed from Table I that the maximum power transfer during night time (850 MW) is actually less than the maximum power transfer value during the daytime (861 MW). This is because of an additional constraint that while increasing the power transfer, the overshoot in PCC voltage should not exceed 1.1 p.u. If the power transfer is allowed until

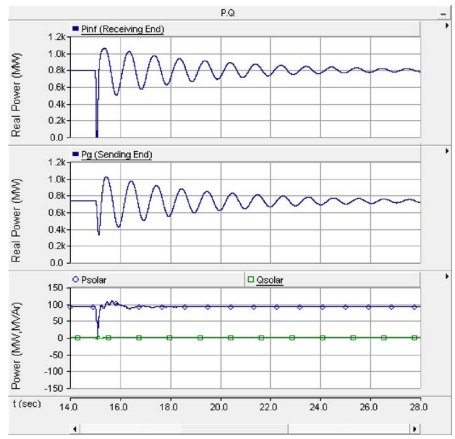


Fig. 5. Maximum daytime power transfer (719 MW) from the generator with solar DG generating 91-MW real power.

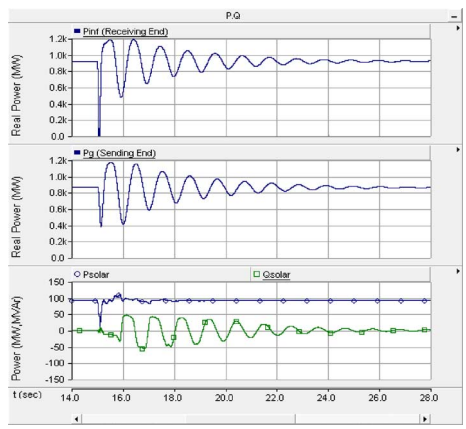


Fig. 6. Maximum daytime power transfer (861 MW) from the generator with solar DG generating 91-MW real power and using the damping controller.

its damping ratio limit of 5% regardless of voltage overshoot, the maximum nighttime power transfer is observed to be 964 MW whereas the maximum daytime power transfer is expectedly seen to be lower at 940 MW (plots not shown).

*2) PCC Voltage Control With the Novel Damping Control:* Transient stability results for a new control strategy involving PCC voltage control, together with damping control, are shown in Table II for the following four cases.

*Solar DG Operation During the Night With a Voltage Controller:* The increase in the power transfer limit depends upon the choice of reference values for PCC voltage $\mathrm{V_{pcc.}}$. In the best scenario when $\mathrm{V_{pcc}}$ is regulated to 1.01 p.u., the maximum power output from the generator increases to 833 MW, compared to 731 MW when the solar DG operates with conventional reactive power control.

*Solar DG Operation During the Day With the Voltage Controller:* The power transfer increases for both low (19 MW) and high (91 MW) power output from the solar farm are seen to be highly sensitive to the PCC bus voltage setpoint. It is also noted that with lower availability of reactive power capacity after real power production, the ability to change the bus voltage is limited, which leads to a lower increase in power transmission capacity.

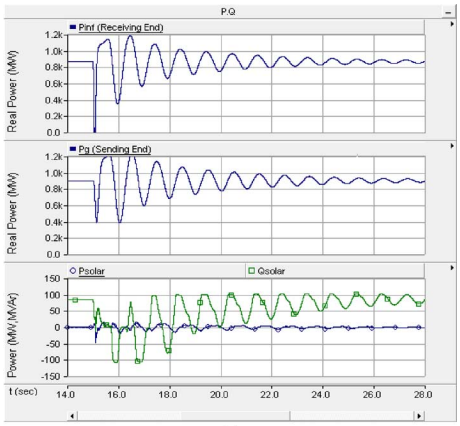


(a)

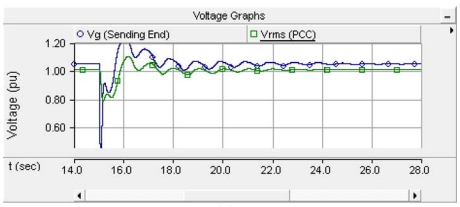


(b)

Fig. 7. (a) Maximum nighttime power transfer (899 MW) from the generator while the solar DG uses a damping controller with voltage control and (b) voltages at the generator terminal and solar DG PCC (1.01 p.u.).

*Solar DG Operation During the Night With Both Voltage and Damping Controllers:* The generator and infinite bus power are depicted in Fig. 7(a), and corresponding voltages are shown in Fig. 7(b). Although, the rotor-mode oscillations settle faster, the power transfer cannot be improved beyond 899 MW due to high overshoot in voltages.

*Solar DG Operation During the Day With Voltage and Damping Controllers:* A further increase in power transfer is observed when both voltage control and damping control are employed, compared to case 2) when only the voltage controller is utilized.

For Study System 1, the net increase in power transfer capability as achieved with different PV-STATCOM controls in comparison with that obtained from conventional reactive power control of the solar DG, is summarized in Table III.

The maximum increase in the power transfer limit during nighttime is achieved with a combination of voltage control and damping control, whereas the same during daytime is accomplished with damping control alone. This is because at night, the entire megavolt-ampere rating of the solar DG inverter is available for reactive power exchange, which can be utilized for achieving the appropriate voltage profile at PCC conducive for increasing the power transfer, as well as for increasing the damping of oscillations.

During daytime, first, the generation of real power from the solar DG tends to increase the voltage at PCC [5] and second, the net reactive power availability also gets reduced especially with large solar real power outputs. Therefore, it becomes difficult with limited reactive power to accomplish the appropriate voltage profile at PCC for maximum power transfer and to impart adequate damping to the oscillations. However, if only damping control is exercised during daytime, power transfer

TABLE IV
POWER FLOWS AND VOLTAGES FOR STUDY SYSTEM II FOR BOTH SOLAR DG AND WIND DG WITH CONVENTIONAL REACTIVE POWER CONTROL AND PROPOSED DAMPING CONTROL BOTH DURING NIGHTTIME AND DAYTIME ($Vg = 1.05$ p.u.)

| Control system | | Gen. Bus | Wind DG at Bus (5) | | Solar DG at Bus (6) | | Inf. Bus |
|---|---|---|---|---|---|---|---|
| | | Pg (MW) | Vwnd (pu) | Pwnd (MW) | Vsol (pu) | Psol (MW) | Pinf (MW) |
| Nighttime ( Psolar = 0 ) | Conventional Control | **Case 1-** None of the DGs generate real power | | | | | |
| | | **731** | 1.019 | 0 | 1.004 | **0** | **-708** |
| | | **Case 2-** Only wind DG generates real power but both DGs operate with conventional reactive power control | | | | | |
| | | **716** | 1.017 | **95** | 1.01 | 0 | **-785** |
| | | **729** | 1.018 | **20** | 1.003 | 0 | **-726** |
| | with damping controller. | **Case 3-** None of the DGs generate real power but both DGs operate with damping control | | | | | |
| | | **960** | 0.998 | -0.7 | 0.982 | -0.2 | **-918** |
| | | **Case 4-** Only wind DG generates real power but both DGs operate on damping control | | | | | |
| | | **936** | 0.995 | **95** | 0.976 | -0.3 | **-987** |
| | | **948** | 0.998 | **20** | 0.981 | -0.7 | **-927** |
| Daytime (Psolar ≠ 0 ) | Conventional Control | **Case 5-** Both DGs generate real power | | | | | |
| | | **700** | 1.016 | **95** | 1.000 | **95** | **-865** |
| | | **726** | 1.019 | **20** | 1.004 | **20** | **-743** |
| | | **Case 6-** Only solar DG generates power | | | | | |
| | | **719** | 1.017 | 0 | 1.002 | **95** | **-790** |
| | | **730** | 1.018 | 0 | 1.003 | **20** | **-727** |
| | with damping controller. | **Case 7-** Both DGs generate real power with damping control. | | | | | |
| | | **930** | 0.99 | **95** | 0.972 | **95** | **-1073** |
| | | **923** | 1.0 | **20** | 0.983 | **20** | **-924** |
| | | **Case 8 -** Only solar DG generates real power but both DGs operate on damping control. | | | | | |
| | | **938** | 0.998 | -0.5 | 0.98 | **95** | **-991** |
| | | **944** | 0.999 | -0.3 | 0.982 | **20** | **-925** |

limits appear to improve with higher real power outputs from the solar DG. This is because real power generation increases the PCC voltage which can be potentially helpful in increasing the power transfer capacity.

Since damping control is found to be more effective during the daytime, the same is explored further for the following studies.

### B. Case Study 2: Power Transfer Limits in Study System II

In this study, the proposed damping control strategy is compared with the conventional reactive power control strategy for Study System II shown in Fig. 1(b). A three-phase-to-ground fault of 5 cycles is applied to the generator bus at $t = 8$ s. The power transfer limits obtained through transient stability studies for different cases are illustrated in Table IV. The following eight cases are studied:

*1) Nighttime:*

*Case 1 – None of the DGs Generate Real Power:* The maximum power transfer limit is 731 MW as in Table I.

*Case 2 – Only Wind DG Generates Real Power. Both DGs Operate With Conventional Reactive Power Control:* The power transfer limit decreases slightly with increasing wind power output.

*Case 3 – None of the DGs Generate Real Power But Both DGs Operate With Damping Control:* The different variables, generator power $P_g$, infinite bus power $P_{inf}$, real power of wind DG $P_{wind}$, reactive power of the wind DG $Q_{wind}$, real power of the solar DG $P_{solar}$, and the reactive power of the solar DG

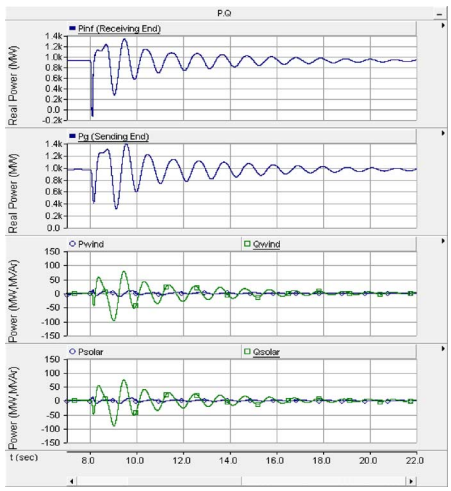


Fig. 8. Maximum nighttime power transfer from the generator with both DGs using the damping controller but with no real power generation.

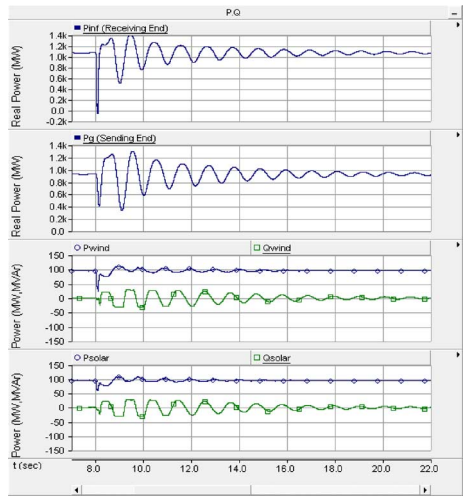


Fig. 9. Maximum daytime power transfer from the generator while both DGs generate 95 MW, each using a damping controller.

$Q_{solar}$ are illustrated in Fig. 8. Even though the entire ratings (100 MVar) of the wind DG and solar DG inverters are not completely utilized for damping control, the power transfer limit increases significantly to 960 MW.

*Case 4 – Only Wind DG Generates Real Power But Both DGs Operate on Damping Control:* There is only a marginal improvement in the power limit with decreasing power output from the wind DG.

*2) Daytime:*

*Case 5 – Both DGs Generate Real Power:* The power transfer limit from the generator decreases as the power output from both DGs increase.

*Case 6 – Only Solar DG Generates Power:* The power transfer limit from the generator decreases as the power output from the solar DG increases. However, no substantial changes in power limits are observed compared to the case when both DGs generate power (Case 5).

*Case 7 – Both DGs Generate Real Power and Operate on Damping Control:* This case is illustrated by different variables $P_g$, $P_{inf}$, $P_{wind}$, $Q_{wind}$, $P_{solar}$, and $Q_{solar}$ in Fig. 9. The power limit does not change much with increasing power output from both DGs.

*Case 8 – Only Solar DG Generates Real Power But Both DGs Operate on Damping Control:* The power limit does not appear to change much with increasing power output from the solar DG.

For Study System 2, the net increases in power transfer limits accomplished with the proposed novel damping control for different real power outputs from both DGs compared to those attained with the conventional operation of both DGs, are depicted in Table V. The proposed damping control on the two DGs (of rating 100 MW each) in the night increases the power transfer limits substantially by about 220 MW. This is expected since in the night, the entire inverter MVA rating of both DGs is available for damping control. The improvement is slightly less when wind DG produces high power. This is also expected as the reactive power availability decreases with the wind DG power output. During daytime, the proposed damping control on both DGs also increases the power transfer limits substantially. A greater increase is seen during high-power generation by any DG, since high power output improves the PCC voltage profile which assists in increasing the power transfer capacity.

TABLE V
INCREASE IN POWER TRANSFER LIMITS FOR STUDY SYSTEM II WITH DIFFERENT DG POWER OUTPUTS

| DG Real Power Outputs (MW) | Power Limit Increase (MW) |
|---|---|
| **NIGHT** | |
| $P_{solar} = 0$; $P_{wind} = 0$ | 229 |
| $P_{solar} = 0$; $P_{wind} = 20$ | 219 |
| $P_{solar} = 0$; $P_{wind} = 95$ | 220 |
| **DAY** | |
| $P_{solar} = 20$; $P_{wind} = 20$ | 197 |
| $P_{solar} = 95$; $P_{wind} = 95$ | 230 |
| $P_{solar} = 20$; $P_{wind} = 0$ | 214 |
| $P_{solar} = 95$; $P_{wind} = 0$ | 219 |

## IV. IMPLEMENTATION OF PV-STATCOM ON LARGE-SCALE SOLAR SYSTEMS

The PV-STATCOM technology will be showcased for the first time in a utility network of Ontario on a 10-kW PV solar system. The 10-kW solar system will be utilized for voltage regulation and power factor correction in addition to generating real power. Several detailed testing and validation studies are required to be completed before the PV-STATCOM will be allowed to connect to the wires of the utility. These include: 1) PV-STATCOM controller testing with PSCAD/EMTDC simulation studies; 2) controller validation using real-time digital simulation (RTDS) [21]; and, finally, 3) a full-scale 10-kW lab-scale demonstration of the PV-STATCOM. Other lab tests would be performed to meet requirements of IEEE standard 1547 [22].

The path for implementing PV-STATCOM technology in large real-scale solar power systems is much more complex than that for the 10-kW systems. Major issues have to examined and addressed. With respect to inverter technologies, adapting

the PV-STATCOM concept to different configurations of inverters: six-pulse, multipulse, multilevel, etc., and control coordination amongst multiple inverters in a PV solar plant, with each operating in PV-STATCOM mode, need to be addressed. Grid connection issues, such as protection and control, voltage rise and harmonics, short-circuit current limitations, disconnection during faults, or staying connected with low-voltage ride-through (LVRT) capabilities, need to be examined. Retrofitting PV inverters in large solar plants with PV-STATCOM technology will have to deal with warranty issues of inverters, in addition to revalidation of the solar system performance with the new PV-STATCOM retrofit. Another aspect is conformance to standards, such as IEEE 1547 and its planned updates.

## V. Practicality of Utilizing Large-Scale Solar Farms for Enhancing Transmission Limits

The number of large solar farms is increasing worldwide. There are at least four operating solar farms of 100-MW rating, three of which are connected at transmission-level voltages [23] with more to follow [24], [25]. The 550-MW Desert Sunlight Solar Farm Project in California will connect to California's existing 500-kV transmission grid [26]. The Grand Renewable Energy Park, ON, Canada, has a 100-MW solar farm connected to the 230-kV transmission line [27]. Meanwhile, several new transmission lines are being constructed worldwide to enhance power transfer capacity in transmission corridors [28]. Examples of new lines for carrying power from renewable sources are the SWIP project [29], CREZ initiative [4], and BPA system [30]. Evidently, these new lines are being constructed due to inadequate power transfer capacity in these corridors. There is therefore a potential opportunity for large-scale solar farms connected to such lines to provide the much needed increase in power transmission capacity to carry power from conventional and renewable energy sources. The concepts presented in this paper can be applied in these scenarios.

## VI. Conclusion

Solar farms are idle during nights. A novel patent-pending control paradigm of PV solar farms is presented where they can operate during the night as a STATCOM with full inverter capacity and during the day with inverter capacity remaining after real power generation, for providing significant improvements in the power transfer limits of transmission systems [31], [32]. This new control of PV solar system as STATCOM is called PV-STATCOM. The effectiveness of the proposed controls is demonstrated on two study SMIB systems: System I has one 100-MW PV-STATCOM and System II has one 100-MW PV-STATCOM and another 100-MW PV-STATCOM or 100-MW wind farm controlled as STATCOM. Three different types of STATCOM controls are proposed for the PV solar DG and inverter-based wind DG. These are pure voltage control, pure damping control, and a combination of voltage control and damping control. The following conclusions are made:

1) In study system I, the power transfer can be increased by 168 MW during nighttime and by 142 MW in daytime even when the solar DG is generating a high amount of real power.
2) In Study System II, the transmission capacity in the night can be increased substantially by 229 MW if no DG is producing real power. During nighttime and daytime, the power transfer can be increased substantially by 200 MW, even when the DGs are generating high real power.

This study thus makes a strong case for relaxing the present grid codes to allow selected inverter-based renewable generators (solar and wind) to exercise damping control, thereby increasing much needed power transmission capability. Such novel controls on PV solar DGs (and inverter-based wind DGs) will potentially reduce the need for investments in additional expensive devices, such as series/shunt capacitors and FACTS.

The PV-STATCOM operation opens up a new opportunity for PV solar DGs to earn revenues in the nighttime and daytime in addition to that from the sale of real power during the day. This will, of course, require appropriate agreements between the regulators, network utilities, solar farm developers, and inverter manufacturers.

## Appendix

Parameters of solar and wind inverter controllers:
PI1: $K_p = 1, T_i = 0.0015$; PI2: $K_p = 1, T_i = 0.1$; PI3: $K_p = 2, T_i = 0.2$; PI4: $K_p = 10, T_i = 0.0015$;
Damping controllers: $T_w = 0.1, G = 1.0, T_1 = 1, T_2 = 0.37$.

## References


[1] R. M. Mathur and R. K. Varma, *Thyristor-Based FACTS Controllers for Electrical Transmission Systems*. Hoboken, NJ, USA: Wiley/IEEE, 2002.

[2] S. A. Rahman, R. K. Varma, and W. Litzenberger, "Bibliography of FACTS applications for grid integration of wind and PV solar power systems: 1995–2010, IEEE working group report," presented at the IEEE Power Energy Soc. Gen. Meeting, Detroit, MI, USA, Jul. 2011.

[3] Y. Xiao, Y. H. Song, C.-C. Liu, and Y. Z. Sun, "Available transfer capability enhancement using FACTS devices," *IEEE Trans. Power Syst.*, vol. 18, no. 1, pp. 305–312, Feb. 2003.

[4] Cross Texas Transmission, Salt fork to gray project. 2014. [Online]. Available: http://www.crosstexas.com/SFWind.htm

[5] R. K. Varma, V. Khadkikar, and R. Seethapathy, "Nighttime application of PV solar farm as STATCOM to regulate grid voltage," *IEEE Trans. Energy Convers.*, vol. 24, no. 4, pp. 983–985, Dec. 2009.

[6] R. K. Varma and V. Khadkikar, "Utilization of solar farm inverter as STATCOM," U.S. Provisional Patent, Sep. 15, 2009.

[7] R. K. Varma, S. A. Rahman, and R. Seethapathy, "Novel control of grid connected photovoltaic (PV) solar farm for improving transient stability and transmission limits both during night and day," in *Proc. World Energy Conf.*, Montreal, QC, Canada, 2010, pp. 1–6.

[8] R. A. Walling and K. Clark, "Grid support functions implemented in utility-scale PV systems," in *Proc. IEEE Power Energy Soc, Transm. Distrib. Conf. Expo.*, 2010, pp. 1–5.

[9] F. L. Albuquerque, A. J. Moraes, G. C. Guimaraes, S. M. R. Sanhueza, and A. R. Vaz, "Photovoltaic solar system connected to the electric power grid operating as active power generator and reactive power compensator," *Solar Energy*, vol. 84, no. 7, pp. 1310–1317, Jul. 2010.

[10] A. Beekmann, J. Marques, E. Quitmann, and S. Wachtel, "Wind energy converters with FACTS Capabilities for optimized integration of wind power into trans. and dist. systems," in *Proc. CIGRE*, Calgary, AB, Canada, 2009.

[11] S. A. Rahman and R. K. Varma, "PSCAD/EMTDC model of a 3-phase grid connected photovoltaic solar system," in *Proc. 43rd North Amer. Power Symp.*, Boston, MA, USA, 2011, pp. 1–5.

[12] K. H. Hussein, I. Muta, T. Hoshino, and M. Osakada, "Maximum photovoltaic power tracking: an algorithm for rapidly changing atmospheric conditions," *Proc. Inst. Elect. Eng., Gen., Transm. Distrib.*, vol. 142, no. 1, pp. 59–64, Jan. 1995.

[13] K. Chatterjee, B. G. Fernandes, and G. K. Dubey, "An instantaneous reactive volt–ampere compensator and harmonic suppressor system," *IEEE Trans. Power Electron.*, vol. 14, no. 2, pp. 381–392, Mar. 1999.

[14] M. H. Rashid, *Power Electronics Handbook*. London, U.K.: Academic, 2001, pp. 355,363–364.
[15] S.-K. Kim, J.-H. Jeon, C.-H. Cho, E.-S. Kim, and J.-B. Ahn, "Modeling and simulation of a grid-connected PV generation system for electromagnetic transient analysis," *Solar Energy*, vol. 83, pp. 664–678, 2009.
[16] A. Yazdani and R. Iravani, *Voltage-Sourced Converters in Power Systems-Modeling, Control and Applications*. Piscataway, NJ, USA: IEEE/Wiley, 2011.
[17] M. F. Schonardie and D. C. Martins, "Three-phase grid-connected photovoltaic system with active and reactive power control using $dq0$ transformation," in *Proc. PESC.*, 2008, pp. 1202–1207.
[18] Z. Ye, R. Walling, L. Garces, R. Zhou, L. Li, and T. Wang, "Study and development of anti-islanding control for grid-connected inverters," GE Global Res. Center, New York, USA, NREL/SR-560-36243, 2004.
[19] P. Kundur, *Power System Stability and Control*. New York, USA: McGraw-Hill, 1994.
[20] "Impact of interactions among power system controls," CIGRE Task Force 38.02.16, France, 2000, CIGRE Tech. Brochure 166.
[21] R. K. Varma, E. Siavashi, B. Das, and V. Sharma, "Novel application of a PV solar plant as STATCOM during night and day in a distribution utility network – Part 2," presented at the IEEE Transm. Distrib. Conf., Orlando, FL, USA, May 2012.
[22] *IEEE Standard for Interconnecting Distributed Resources With Electric Power Systems*, Standard 1547-2003.
[23] PV Resources, Large scale photovoltaic power plants ranking 1-50, 2014. [Online]. Available: http://www.pvresources.com/PVPowerPlants/Top50.aspx
[24] U.S. Dept. Energy, Media release, Jun. 30, 2011. [Online]. Available: http://energy.gov/articles/department-energy-offers-conditional-loan-guarantee-commitments-support-nearly-45-billion
[25] First Solar, Desert sunlight solar farm, 2014. [Online]. Available: http://www.firstsolar.com/en/about-us/projects/desert-sunlight-solar-farm
[26] Desert Sunlight Holdings, Desert sunlight solar farm project draft EIS and CDCA plan amendment, 2010. [Online]. Available: http://www.blm.gov/pgdata/etc/medialib/blm/ca/pdf/palmsprings/desert_sunlight.Par.38926.File.dat/Chapter-2.0_Project-Description-Draft-EIS-DesertSunlightSolarProject.pdf
[27] Stantec Consulting Ltd., Grand renewable energy park construction plan report, 2011. [Online]. Available: http://www.samsungrenewableenergy.ca/sites/default/files/pdf/GREP_ConstructionPlanReport.pdf
[28] Global Transmission, Project update: North America, Global Transm. Rep., 2014. [Online]. Available: http://www.globaltransmission.info/archive_main.php?id=18&region=1
[29] Great Basin Transmission LLC, Southwest Intertie Project, 2011. [Online]. Available: http://www.swipos.com/about.htm
[30] Bonneville Power Administration, "BPA to build new high-voltage power line in Southeast Washington," *Transm. Distrib. World Mag.* May 2011. [Online]. Available: http://tdworld.com/overhead-transmission/bpa-build-new-high-voltage-power-line-southeast-washington
[31] R. K. Varma and S. A. Rahman, "Novel control of inverter based DGs as FACTS (DGFACTS) for enhancing grid power transmission limits," U.S. Provisional Patent No. 61/309,612, Mar. 2, 2010.
[32] R. K. Varma, V. Khadkikar, and S. A. Rahman, "Utilization of distributed generator inverters as STATCOM," Canada PCT Patent appl. PCT/CA2010/001419, Sep. 15, 2010.

**Rajiv K. Varma** (SM'09) received the B.Tech. and Ph.D. degrees in electrical engineering from the Indian Institute of Technology (IIT), Kanpur, India, in 1980 and 1988, respectively.

Currently, he is Associate Professor and Hydro One Chair in Power Systems Engineering at the University of Western Ontario (UWO), London, ON, Canada. Prior to this position, he was a faculty member in the Electrical Engineering Department, Indian Institute of Technology, Kanpur, India, from 1989 to 2001. He has co-authored an IEEE Press/Wiley book on thyristor-based FACTS controllers. He has co-delivered several tutorials on SVC sponsored by the IEEE substations committee. His research interests include flexible ac transmission systems, power systems stability, and grid integration of wind and photovoltaic solar power systems.

Prof. Varma is active on a number of IEEE working groups. He was a member of the IEEE Working Group on "HVDC and FACTS Bibliography and Records" during 1994–1998. He been the Chair of IEEE Working Group 15.05.17 on "HVDC and FACTS Bibliography," since 2004.

**Shah Arifur Rahman** (M'13) received the Ph.D. degree in electrical power systems engineering from the University of Western Ontario, London, ON, Canada.

Currently, he is a Postdoctoral Fellow with the university and performs research activities at Bluewater Power, Sarnia, ON. His research interests include grid integration of inverter-based distributed-generation (DG) sources, such as photovoltaic solar plants, wind farms, energy storage, impact analysis of harmonics and overvoltages on power systems, implementation of flexible ac transmission systems, as well as the capability in inverter-based DGs and their coordination.

Dr. Rahman is a member of the IEEE Working Group on "HVDC and FACTS Bibliography and Records" since 2010 and is Acting Secretary since 2012.

**Tim Vanderheide** (M'14) is Chief Operating Officer for Bluewater Power Renewable Energy Inc. and Electek Power Services Inc., Sarnia, ON, Canada. He is also Vice President of Strategic Planning for Bluewater Power Distribution Corporation and is responsible for the development and implementation of renewable power generation projects for Bluewater Power Renewable Energy Inc. as well as the development of new product and service strategies designed to continuously improve shareholder value for Bluewater Power Distribution. In his role as Chief Operating Officer for Electek Power Services Inc., he is responsible for overall operations and company growth. Prior to his current positions, he was Vice-President of Client Services for Bluewater Power Distribution Corporation. In this role, he was responsible for market services, energy services, metering, billing, and information technologies.